5-2017

Myosin XI-I works in tandem with a microtubule-associated mechanism to position the nucleus in Arabidopsis root hairs

Ian Andrew Windham
iwindham@vols.utk.edu

Myosin XI-I works in tandem with a microtubule-associated mechanism to position the nucleus in *Arabidopsis* root hairs

By

IAN A. WINDHAM

Advisor: Andreas Nebenführ

May 2016

An Honors Thesis

Presented to the Faculty of the

Department of Biochemistry and Cellular and Molecular Biology

& the Chancellor's Honors Program

University of Tennessee, Knoxville

In Partial Fulfillment of the

Requirements for the Degree of

Bachelor of Science

Abstract

Myosins are an extensive superfamily of molecular motor proteins, wherein class XI myosins are encoded solely in plants and typically function in rapid intracellular transport along actin filaments. Intracellular transport is especially important in the polarized cell growth exhibited by root hairs, which are extensions of single epidermal root cells. In *Arabidopsis thaliana*, the atypical myosin XI-I binds to the WIT-WIP complex on the outer nuclear envelope. The shape of the nucleus in *xi-i* mutants is rounded and invaginated, and certain nuclear movements are diminished. The nucleus of growing root hairs maintains a relatively fixed difference from the tip. Previous work has pointed to actin filaments as the primary driver of nuclear positioning in the growing root hair. Thus, we hypothesized that actin-bound myosin XI is required for nuclear positioning in *Arabidopsis* root hairs.

Nuclear position relative to the root hair tip in *xi-i* is more variable than in wild-type, although the overall mean distance from the tip is not significantly different. *xi-i* nuclei were also more circular, exhibiting a rounded morphology more frequently than in wild-type. However, there is no significant difference in the rate of root hair growth between genotypes. Interestingly, disruption of microtubule polymerization by treatment with 5 μM oryzalin resulted in a marked increase in the variability of root hair nucleus position. This implies a yet uncharacterized mechanism involving microtubules as well as myosin XI-I in nuclear position and shape. However, considering the position of the nucleus does not appear to be important for root hair growth, why such a mechanism is necessary is still not understood.

Table of Contents

Introduction

Class XI myosins are an atypical family of cytoskeletal motor proteins that drive the rapid, processive transport of organelles and vesicles responsible for the cytoplasmic streaming observed in plant cells (Madison & Nebenführ, 2013). Myosin XI is a plant-specific homolog of myosin V, which transports organelles and vesicles in animal and fungal cells (Li & Nebenführ, 2008). Both myosin XI and myosin V possess a motor head domain that utilizes energy from ATP hydrolysis to power movement along actin filaments and a globular tail domain that facilitates binding to cargo such as vesicles or organelles (Li & Nebenführ, 2007). Most plants encode a number of myosin XI isoforms; there are thirteen in *Arabidopsis thaliana*. Interestingly, the globular tail domain varies among the 13 myosin XI isoforms encoded in *Arabidopsis*, suggesting that different isoforms bind to different cargo to perform specific functions (Li & Nebenführ, 2008).

Myosin XI-I is the most phylogenetically distant of the class XI myosins found in *Arabidopsis* (Tominaga & Nakano, 2012). *In vitro* studies show that the actin-sliding velocity of XI-I is more than ten times slower than that of other isoforms of myosin XI, primarily due to a high affinity for ADP (Haraguchi et al., 2016). This suggests that myosin XI-I is not involved in rapid organelle transport. Indeed, it was found that the globular tail domain of XI-I binds to WIT-WIP protein complexes on the nuclear envelope. In *xi-i* mutants, the nuclear envelope is more rounded and invaginated, and the dark-induced positioning of the nucleus to the periclinal wall in mesophyll cells is diminished (Tamura et al., 2013). These results suggest that myosin XI-I plays an important role in nuclear shape and movement. This actomyosin nuclear positioning complex contrasts with mechanisms found in animals, which utilize microtubule bound motor proteins to maintain shape and position (Star & Fridolfsson, 2010).

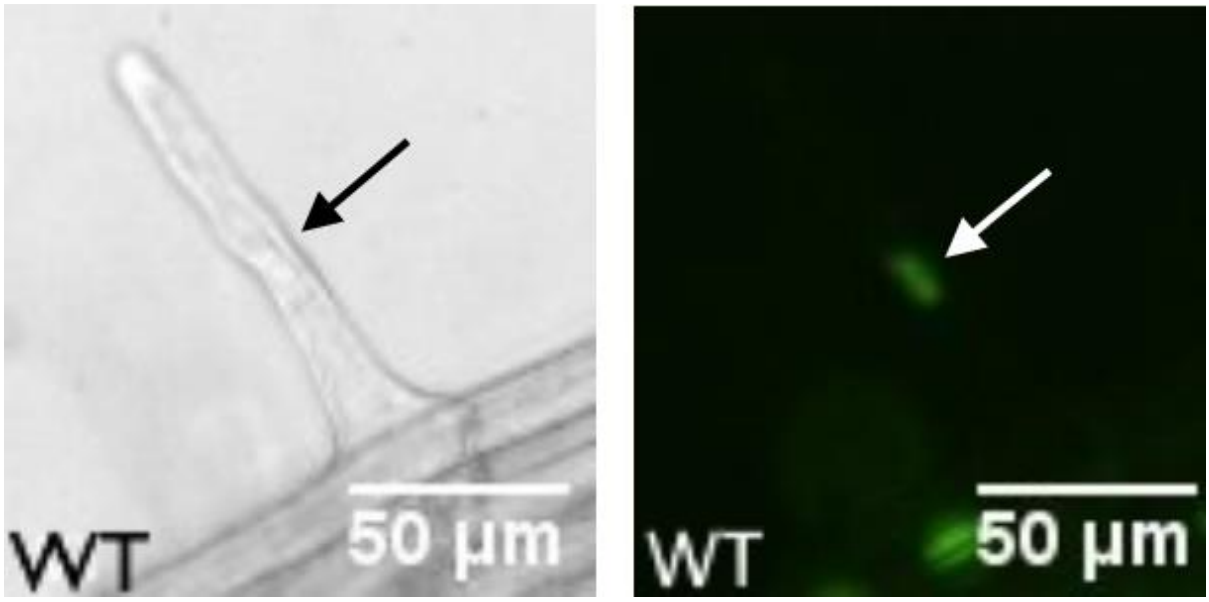

Figure 1: An *Arabidopsis* root hair at 10x magnification. The arrow points to the location of the nucleus.

Root hairs are extensions of root epidermal cells, called trichoblasts, that exhibit highly polarized growth, expanding only at the tip. This growth is dependent on the rapid intracellular transport of organelles and secretory vesicles along actin filaments to the apex of the root hair (Cole & Fowler, 2006). The nucleus of a root hair maintains a relatively fixed distance from the tip during growth. When root hairs are fully grown, the nucleus migrates to a random position in the cell (Ketelaar et al., 2002). These authors posit that the position of the nucleus is determined primarily by the actin cytoskeleton, since microtubules were shown to play a minimal role in the position of the root hair nucleus. Maintaining nuclear position during growth is thought to play an important role in facilitating polarized cell growth, as blocking nuclear movements with optical tweezers arrests root hair growth (Ketelaar et al., 2002).

Observations of nuclear the trichoblasts of ROP2 GTPase overexpressing plants, which exhibit multiples root hairs emerging from the same cell, contradict the conclusions made by Ketelaar et al. (2002). In these multiple root hair cells, the nucleus remains close to one of the

growing root hair tips while the other grows at the same rate without a nucleus (Jones & Smirnoff, 2006). This result implies that root hair growth is independent of the position of the nucleus, as root hairs lacking a nucleus grow at the same rate.

Nuclear positioning in *Arabidopsis* root hairs is thought to depend on actin filaments rather than microtubules (Ketelaar et al., 2002). Myosin XI-I connects the nuclear envelope to the actin cytoskeleton, and is required for proper nuclear shape and dark-induced nuclear positioning (Tamura et al., 2013). Taken together, these results suggest that actin-bound myosin XI-I is the primary determinant of nuclear shape and position. Thus, we hypothesize loss of myosin XI-I function should affect the positioning of the nucleus in growing root hairs. If nuclear positioning is maintained after complete XI-I loss of function, then other mechanisms must be in place that position the nucleus in tandem with myosin XI-I. The effect of disrupting nuclear positioning mechanisms on root hair growth is difficult to infer given the conflicting results described above. However, if a sophisticated mechanism precisely controlling the position of the nucleus during root hair growth has evolved in *Arabidopsis*, then we would expect to see an effect on normal root hair growth when nuclear positioning is disrupted.

Methods

Isolation of homozygous *xi-i* knockout lines

Genomic DNA was extracted from *Arabidopsis* lines putatively carrying the myosin *xi-i* T-DNA insertional knockout alleles SALK_029565 and SALK_092026, hereafter referred to as *iT1* and *iT3* respectively, for genotyping (Alonso et al., 2003). Plants were grown to the rosette stage, and single leaves were harvested and ground in an extraction buffer containing 200 mM Tris-Cl, 250 mM NaCl, 25 mM EDTA and 0.5% SDS. The mixture was vortexed and allowed to

sit at room temperature before being centrifuged for ten minutes to separate the supernatant containing the gDNA from the pellet of insoluble plant tissue. The supernatant was separated from the pellet and mixed with an equal volume of isopropanol. After 10 minutes of centrifugation, the supernatant was discarded and 95% ethanol was used to wash the pellet to remove any remaining impurities. Distilled water was added to the dry pellet containing the gDNA. Samples were stored at -20 C.

Polymerase chain reaction (PCR) was used to determine the presence of the *iT1* or *iT3* alleles. Mixtures were prepared consisting of 2 mM deoxynucleotide triphosphates, a standard 10x Taq buffer, two 12.5 μM DNA primers, and Taq polymerase. These mixtures were combined with 1 μM of each gDNA sample of interest and gently mixed before being placed in a thermal cycler. Two separate primer pairs were used to analyze each gDNA sample. One primer pair, hereafter referred to as the "wild-type" pair, defines a region of DNA at the T-DNA insertion site for the allele of interest that is approximately 1000 base pairs long. These primers are referred to as the left primer (LP) and the right primer (RP) for the insertion site. The second primer pair, the "mutant" pair, consists of a T-LBb primer complementary to one end of the inserted T-DNA fragment and either the LP or RP primer of corresponding the insertion site, depending on the orientation of the insertion. Table 1 lists the primer sequences utilized in genotyping the putative *iT1* and *iT3* lines, and Table 2 details annealing temperatures, extension times, and the number of cycles used in PCR.

PCR products were subsequently analyzed using gel electrophoresis to verify the presence of the mutant allele. After each PCR, a 1% agarose in 1x TAE buffer solution was prepared and allowed to dry. The top row of each gel was filled with the PCR products amplified with the wild-type primer set, and the bottom row was filled with product amplified from the

mutant primer set. For each experiment, gDNA from a known wild-type plant (WT) was amplified with both primers pairs as a control. Gels were run at 100 V for 30 minutes and stained in ethidium bromide.

Table 1: Primer sequences used in genotyping PCR

Primer	DNA Sequence
iT1-LP	5’ TGA GGT TGC GCC AGA GAA TTT 3’
iT1-RP	5’ TGT ACG TGG TTG ATG ATA TTG TTG C 3’
iT3-LP	5’ TGC TTC ATT AGC AAC CTG CAA GA 3’
iT3-RP	5’ CTT CAT CTC TGC ACG GGC TTC 3’
T-LBb-1	5’ GCG TGG ACC GCT TGC TGC AAC T 3’

Table 2: PCR parameters for primer pairs used in genotyping

Primer Pair	Annealing Temperature (°C)	Extension Time (seconds)	Number of Cycles
iT1-RP + T-LBb-1	56	90	35
iT1-RP + T-LBb-1	56	90	35
iT3-LP + iT3-RP	54	90	35
iT3-RP + T-LBb-1	56	90	35

Introduction of fluorescent nuclear marker to *xi-i* knockout line *iT3*

To facilitate the observation of root hair nuclei *in vivo*¸ a fluorescent nuclear marker was introduced into both wild-type *A. thaliana* and the previous isolated *xi-i* T-DNA insertional knockout line *iT3* via *Agrobacterium*-mediated transformation. *iT3*, which will hereafter be referred to as *xi-i,* was selected for transformation because it is the same SALK line (SALK_092026) as the *kaku1-3* line in the paper by Tamura et al. (2013). The marker used was a construct consisting of a 35S promoter, a C-terminal β-glucuronidase enzyme (GUS), a nuclear localization signal (NLS), and a N-terminal yellow fluorescent protein(YFP) (Li et al., 2009). Both wild-type and *xi-i Arabidopsis* plants were grown in individually in small pots under long day conditions until flowering. The shoot meristems, as well as any siliques, were removed to maximize transformant yield. An overnight liquid culture was prepared of the *Agrobacterium* strain containing the YFP-NLS construct as well as a selectable marker gene for hygromycin resistance on a binary vector. Plants were then transformed using the standard floral dip protocol, in which the aerial organs of *A. thaliana* plants are coated in *Agrobacterium* culture (Clough & Bent, 1998). T_0 plants were then grown normally until dry and ready for harvesting.

After harvesting, T_1 seeds were sterilized in a 30% bleach, .1% Triton X-100 solution. Sterilized seeds were plated on selection plates with a medium consisting of 50mg/ml hygromycin, 1/4x MS salts, and 1% sucrose at a pH of 5.7 and vernalized at 4 °C before being transferred to 22°C growth chambers. Seedlings were grown under long day conditions (16 hours light, 8 hours dark) for approximately three days, at which point successful transformants typically developed cotyledons. Germinated seedlings were transferred to vertical phytagel plates (1/4x MS salts, 1% sucrose, pH 5.7) and grown 1-2 more days. T_1 seedlings were screened for YFP-fluorescence using a Zeiss Axiovert 200M fluorescence microscope equipped

with filters for YFP. Seedlings exhibiting YFP fluorescence were transferred to soil and grown normally under long day conditions until harvesting. Approximately 24 T_2 seeds from each T_1 plant were sterilized, grown on vertical plates, and screened for fluorescence a second time. Lines exhibiting strong YFP fluorescence throughout the root were used for subsequent imaging.

Imaging and Analysis of Root Hair Nuclei

Select T_2 seeds were sterilized as described above, plated on vertical phytagel plates, and stratified at 4°C for two days. Plates were transferred to 22°C growth chambers and grown under long day conditions. After four days, seedlings were prepared for imaging in small circular chambers with a cover slip bottom containing a small amount of H_2O, with a phytagel blanket (1/4x MS, 1% sucrose, pH 5.7) placed over the root. Seedlings imaged in these chambers will hereafter be referred to as treated under "standard conditions". Other seedlings were placed in cover slip chambers for drug treatment. These chambers consisted of a 22mm x 50mm cover slip base on which the seedling rested in the necessary liquid medium, two vacuum grease coated half 22mm x 22mm on either side of the seedling and another 22mm x 22mm cover slip resting on top. This chamber suspends the root of the seedling in the desired liquid medium while minimizing mechanical stress to the plant and reducing evaporation. Seedlings were first placed in chambers containing a 0.05% solution of DMSO in liquid MS media and imaged over a twenty-minute period. The medium was then removed from the chamber via a paper towel as 60 µL of 5 µM oryzalin in liquid MS media was pipetted in simultaneously. Approximately two to three of these exchanges were performed, and the seedlings were then imaged again for another twenty-minute period.

Root hairs were observed using a Zeiss Axiovert 200M microscope equipped with filters for YFP fluorescence (Zeiss). Openlab5 software was used to capture images both at 10x magnification over 20 minutes at 1 minute intervals and at 40x magnification over 20 minutes at 30 second intervals (Improvision/Perkin Elmer). Images were only used for analysis if the root hair remained growing throughout the entire period of imaging. Measurements were taken in ImageJ, and data was analyzed in RStudio via the tidyverse package (Schneider et al., 2012; RStudio Team, 2015; Wickham, 2017). All plots were made using ggplot2 (Wickham 2009).

The shape of nuclei was measured by setting the threshold range to match the fluorescent signal of the nuclei and then using "Analyze Particles" to automatically measure the circularity index of a selected nucleus. The circularity index is calculated in ImageJ, and derived from the equation 4π *Area/(perimeter)^2. For the seedlings subject to standard growth conditions the distance from the nucleus to the root hair tip was measured at one minute intervals over each twenty-minute period imaged (both 40x and 10x image stacks were included together in all subsequent analysis), and the mean distance for each nucleus was calculated. Additionally, the variance in the distance of the nucleus from the root hair tip for each cell was calculated over the twenty-minute period. For the seedlings treated with oryzalin, the nuclear position relative to the tip was measured every minute before and after treatment. Because time taken to perform the treatment was minimal, the post-treatment nuclear position can be considered continuous with the pre-treatment position. The mean nuclear position for each cell of both genotypes was calculated and set as 0. This pre-treatment mean was then subtracted from the nuclear distance from the tip at each time point before and after oryzalin treatment.

Results

Confirmation of *iT1* and *iT3* homozygotes

The left gel in Figure 2 shows the products of the PCR testing several putative mutant lines for the presence of the *iT1* insertion, as well as a WT control. 500 base pair fragments were amplified for each product using the mutant primer pair. Conversely, no fragment amplified in PCR when the wild-type primer pair was used. This indicates that plants were all homozygous for the insertion allele, and seeds from plants iT1 10B and 11B were kept. The right of Figure 2 shows a gel screening for the *iT3* insertion allele, and shows that a 500 base pair fragment amplified for all four plants using the mutant primer pair. No fragments amplified when using the wild-type primer pair, confirming that the plants were homozygous for the *iT3* allele. Seeds from homozygotes 5A and 5C were kept.

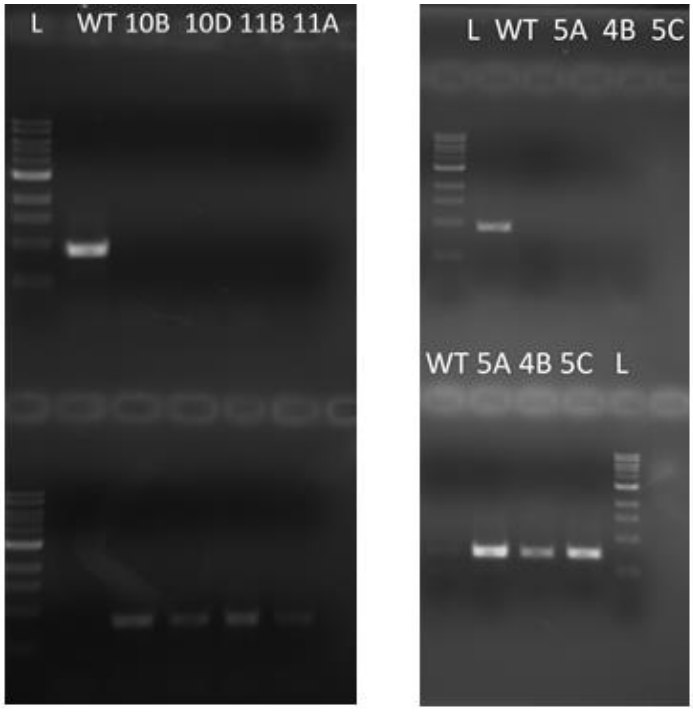

Figure 2: Gels confirming homozygous lines for *iT1* (left) and *iT3* (right). L indicates the 1 kb DNA ladder used for scale.

xi-i nuclei typically exhibit a more circular morphology

To fully characterize how loss of myosin XI-I function affects nuclear shape in *Arabidopsis* root hairs, we compared the morphologies of WT and *xi-i* root hair nuclei. Nuclei in the growing root hairs of WT and *xi-i* displayed a spectrum of shapes. Typically, *xi-i* nuclei were observed with the rounded, irregular morphology seen in Figures 3A and 3C, while WT nuclei exhibited a more elongated, spindle-like shape seen in Figures 3B and 3D. However, the distinction was not always as explicit among all root hairs of the respective genotypes, as previous published data has implied (Tamura et al., 2013). WT nuclei in growing root hairs could also take on a more round, irregular shape (Figure 3E), and *xi-i* nuclei were often elongated (Figure 3F). Figure 4 shows the cumulative distributions of WT and *xi-i* nuclear shape. Consistent with previous observations, *xi-i* root hair nuclei were significantly more circular compared to WT: the mean circularity index of nuclei in growing WT root hairs was 0.474±0.107 compared to 0.558±0.142 in *xi-i* root hairs (p-value 0.0298, Kolmogorov-Smirnov test). Interestingly, the two lines overlap at lower circularity indices, indicating that *xi-i* can have nuclei that are just as elongated as in WT. Despite these variations, the predominance of the circular morphology in *xi-i* supports the role of myosin XI-I as a regulator of nuclear shape in *Arabidopsis* root hairs.

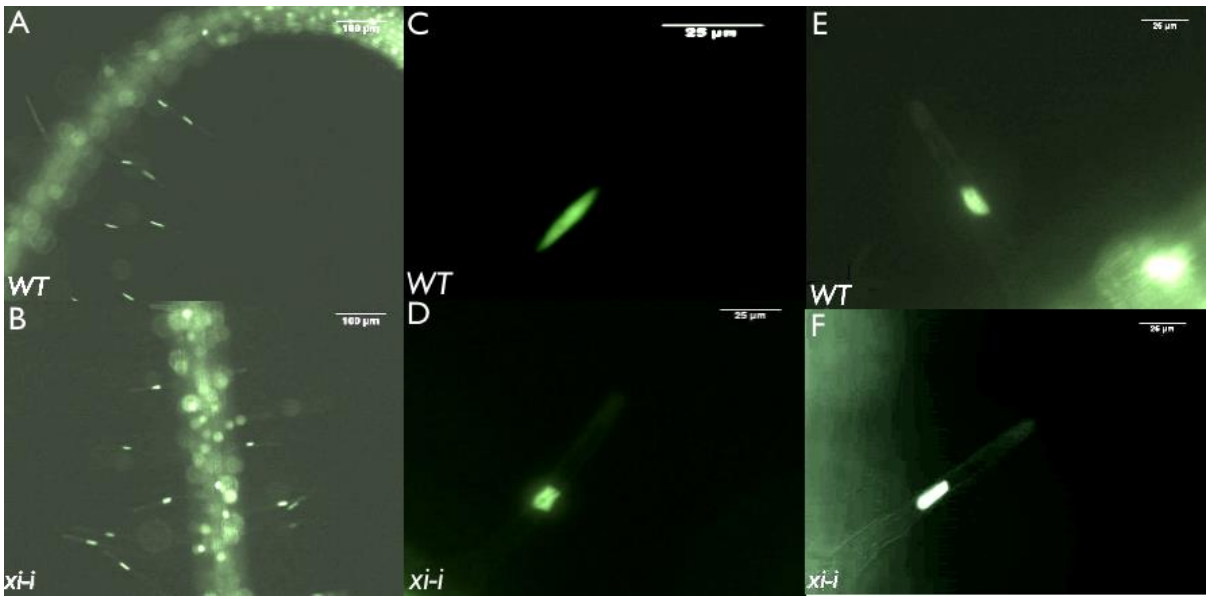

Figure 3: 10x and 40x images of the typical elongated nuclear shape seen in WT root hairs (A; C), and the irregular, rounded shape seen in *xi-i* root hairs (B; d). WT nuclei can also exhibit more irregular morphologies (E), and *xi-i* can be more elongated (F).

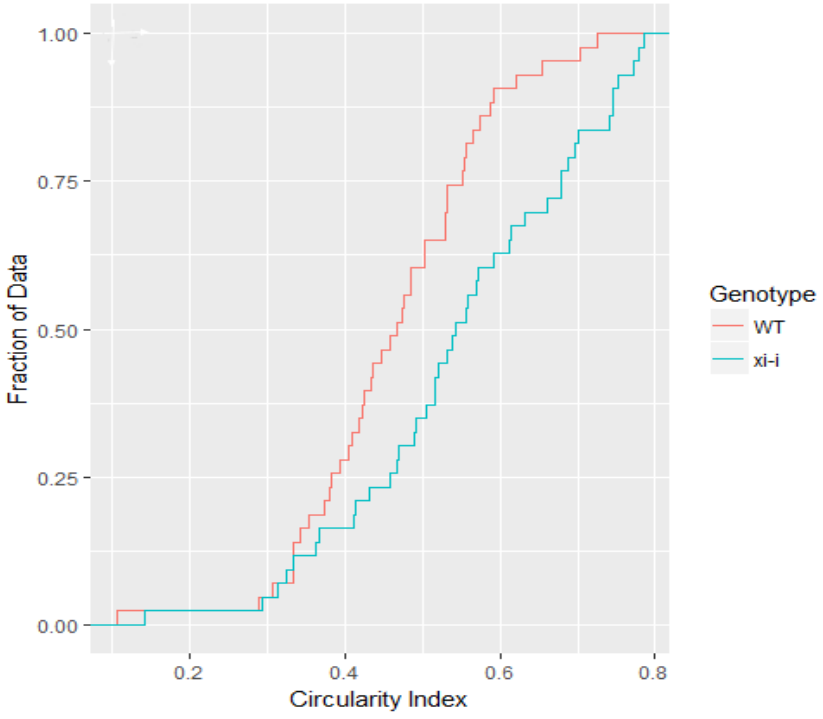

Figure 4: *xi-i* nuclei are typically less circular than WT. (A) shows a cumulative distribution of nuclear shapes (calculated via the circularity index) in WT and *xi-i* (N=41, p value < 0.05, Kolmogorov-Smirnov Test).

_xi-i_ mutants exhibit greater variation in nuclear position, but root hair growth is unaffected

We hypothesized that loss of myosin XI-I function would significantly affect the ability of the nucleus to position itself relative to the growing root hair tip. Therefore, we compared the position of the nucleus in growing root hairs over time in both WT and *xi-i*. Kymographs of nuclear movement in WT (Figure 5A) and *xi-i* (Figure 5B) root hairs over twenty-minutes show distinct differences in the position of the growing root hair nucleus relative to the tip over time. In WT, the nucleus maintained a constant distance from the tip over the course of twenty minutes (Figure 5A). The *xi-i* nucleus shown in Figure 5B had a much more variable position, at first rapidly moving closer to the root hair tip before oscillating around a spot further away from the tip. The mean distance from the nucleus to the tip over twenty minutes was not significantly different in *xi-i* (60.0 µm ± 8.8) compared to WT (61.3 µm ± 25.2) (Figure 5C). However, the variance in position over twenty minutes was much greater in *xi-i,* with a mean variance of 14.54 ± 7.77 compared to a mean variance of 9.84 ± 5.90 in WT (Figure 5D). Nuclei were still able to maintain a similar mean distance from the root hair tip in *xi-i,* but nuclear position from minute to minute was significantly more erratic and variable than in WT.

The necessity of nuclear positioning for normal root hair growth is still poorly understood. Thus, root hair growth rates in both WT and *xi-i* were analyzed in order to determine whether the defects in nuclear positioning caused by loss of myosin XI-I function correlated with slower root hair growth. Under standard conditions, there was no significant different in the rate of root hair growth between WT and *xi-i* (Figure 6). These results corroborate the conclusions made by Jones & Smirnoff (2006) that suggests root hair growth is not dependent on the location of the nucleus.

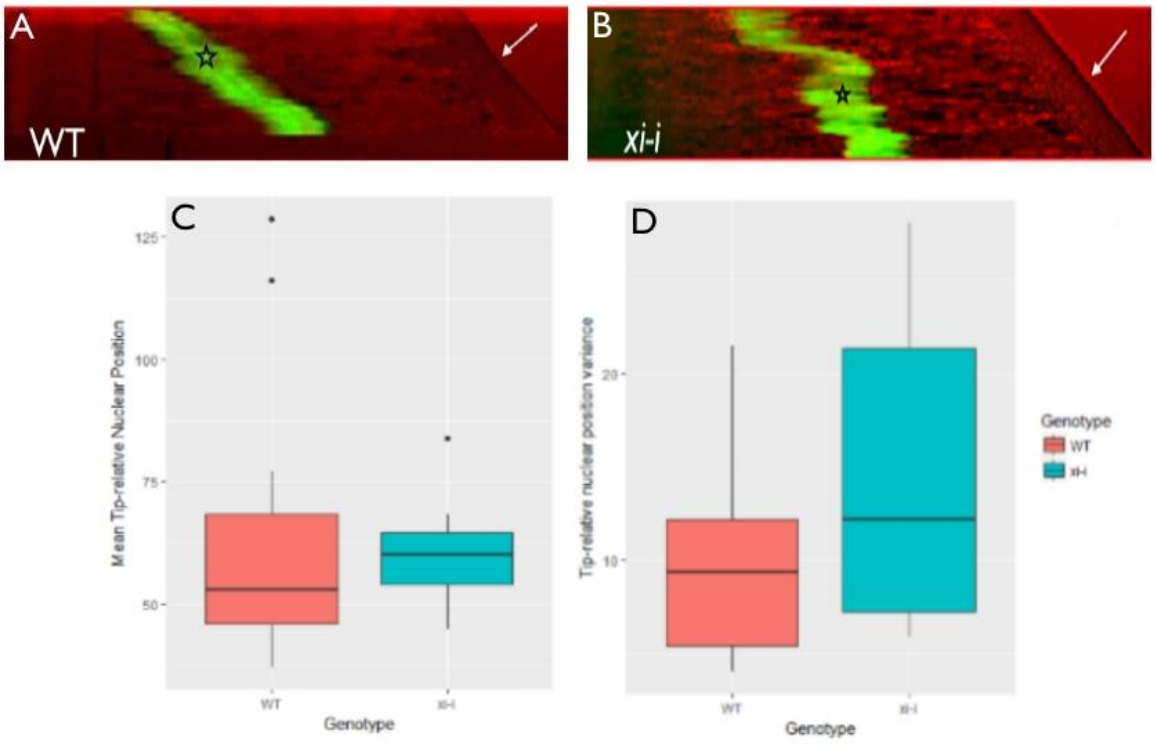

Figure 5: Average nuclear position is maintained, but more variable in *xi-i* root hairs. The kymographs in (A) and (B) show the movement of the nucleus (black star) with respect to the root hair tip (white arrow) over a twenty-minute period in WT and *xi-i* respectively (C) There is no significant different between *xi-i* and WT in the mean position of the nucleus relative to the growing root hair tip over twenty minutes (N=18, p-value = 0.491, two-sided t-test). (D) The variance of the nuclear position over each twenty-minute period is significantly higher in *xi-i* (N:14, p-value = 0.02509, two-sided t-test).

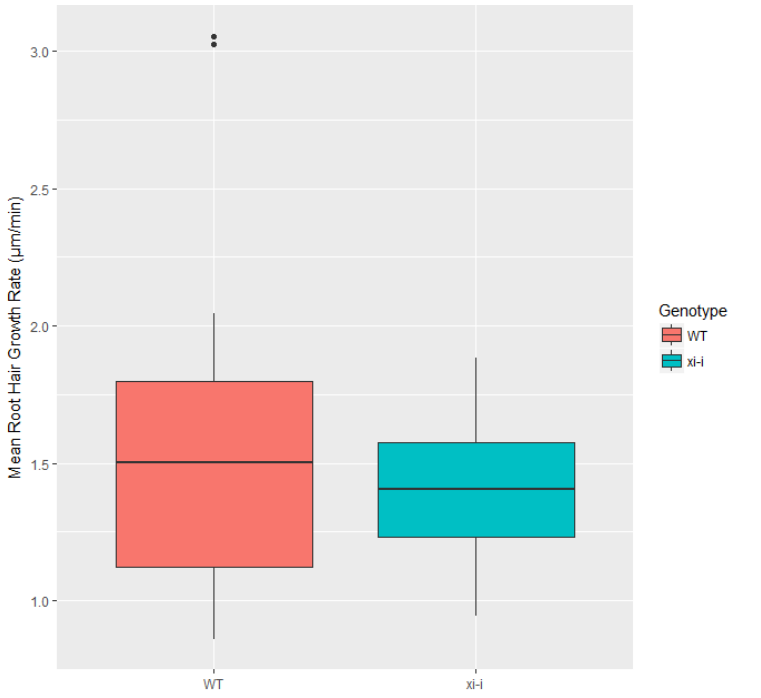

Figure 6: There is no significant difference in growth rate between WT and *xi-i* under standard conditions (N=19, p-value = 0.1815, two-sided t-test)

Nuclear position in *xi-i* is significantly more variable after oryzalin treatment

Loss of myosin XI-I by itself did not significantly affect nuclear positioning in root hairs. Assuming myosin XI-I is the primary linker of the nucleus to the actin cytoskeleton, then other cytoskeletal factors could be involved *xi-i* nuclear positioning. Therefore, we disrupted microtubule polymerization with the drug oryzalin in both WT and *xi-i* and measured the position of the nucleus over time.

The position of nuclei in growing WT root hairs became much more variable after treatment with oryzalin, with a general tendency to move further away from the tip. The

kymograph in Figure 7A shows the increased variability in WT nuclear position after oryzalin treatment. By contrast, nuclear position in growing *xi-i* hairs was widely variable after treatment Some *xi-i* nuclei moved closer to the base, while others positioned closer to the tip. Figure 7B represents the former case, with the nucleus erratically moving back towards the root hair base. Figure 7C shows the position of the nuclei relative to the pre-treatment mean over time, both before and after treatment. Distances closer to the tip than the mean were negative, and distances closer to the base than the mean were positive. The stark increase in the variability of nuclear position after disrupting microtubule polymerization in *xi-i* suggests that microtubules function to position the nucleus in the absence of myosin XI-I.

Figures 7D and 7E show the growth of WT and *xi-i* root hairs, before and after oryzalin treatment. In both the pre-oryzalin DMSO mock treatment and the 5 µm oryzalin treatment, there was again no significant difference in the root hair growth rate between WT and *xi-i.* However, oryzalin treatment resulted in a significant decrease in growth rates for both WT and *xi-i* root hairs (Figure 7F). This is inconsistent with previous research claiming that oryzalin treatment at this concentration does not affect root hair growth rates (Bibiokova et al., 1999). One possible conclusion is that variations in nuclear position caused by oryzalin treatment could be causing a decrease in growth rates. However, slowed root hair growth could also be due to stress from the media exchange.

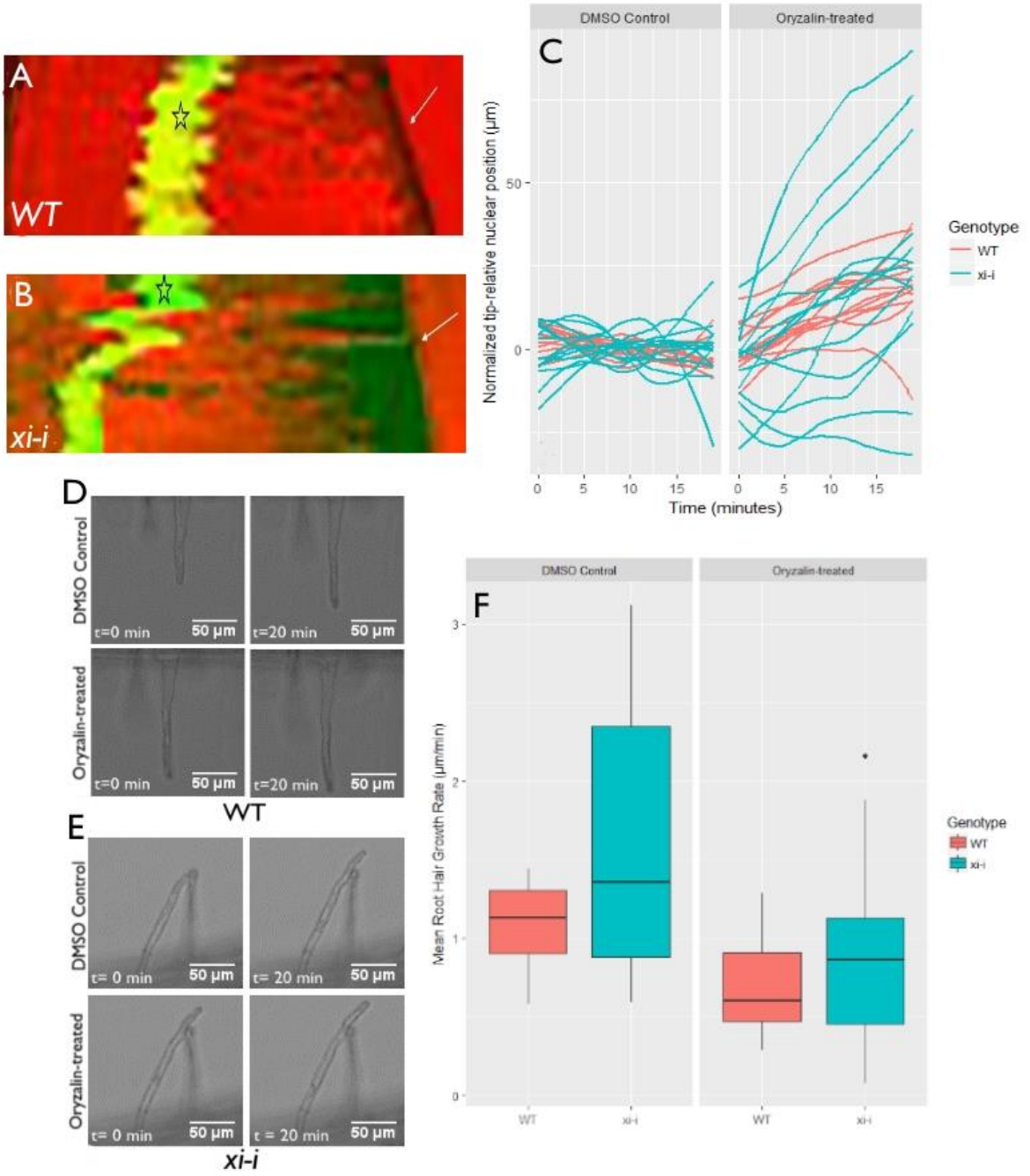

Figure 7: Effects of oryzalin treatment on nulear positioning and root hair growth in WT and *xi-i*. The kymographs in (A) and (B) are representative of the behavior of nuclei after oryzalin treatment in WT and *xi-i* respectively. (C) is a plot of nuclear position relative before and after treatment, relative to the pretreatment mean. (D) and (E) show root hair growth over twenty minutes, before and after oryzalin treatment, in WT and *xi-i* respectively. (F) compares the root hair growth rates of WT and *xi-i* before and after treatment. There is no significant difference in growth rate pre-treatment, (N=13, p-value = 0.064) and after 5 µM oryzalin treatment (N=13, p-value = 0.26). However, growth rates diminish significantly in both genotypes upon oryzalin treatment (N=13, p-value <-0.05).

Discussion

Previously published work has presented data indicating that actin filaments are responsible for positioning the nucleus in *Arabidopsis* root hairs (Ketelaar et al., 2002). Myosin XI-I links the nucleus to the actin cytoskeleton, and loss of XI-I causes defects in nuclear positioning (Tamura et al., 2013). Therefore, we first hypothesized that XI-I is the primary determinant of nuclear positioning in *Arabidopsis.* In *xi-i* nuclei, there was greater variance in the position of the nucleus relative to the tip over twenty minutes than in WT nuclei. However, *xi-i* nuclei were nonetheless able to maintain the same mean distance from the root hair tip as WT. We concluded that other factors besides XI-I must be involved in positioning the nucleus. Disrupting the polymerization of tubulin monomers in wild-type *Arabidopsis* via oryzalin treatment showed increased variability in nuclear position. However, this change was much stronger in oryzalin-treated *xi-i,* in which the position of the nucleus was highly variable, moving either towards the base or the tip of the root hair.

Under standard conditions, there was no significant difference between WT and *xi-i* root hair growth rates. Oryzalin treatment appeared to diminish root hair growth rates in both WT and *xi-i* to a similar degree. However, there was still no significant different in root hair growth rates between WT and *xi-i* root hairs either before or after treatment. There was no difference in growth rates between the two genotypes under any condition, even though nuclear positioning in *xi-i* was more greatly affected than in WT. This indicates that root hair growth is independent of the position of the nucleus, as suggested by Jones & Smirnoff (2006).

The severe defects in nuclear positioning observed in oryzalin treated *xi-i* root hairs indicates that both microtubules and myosin XI-I are necessary for nuclear positioning. This

effect has not been observed in previous research because treatment of wild-type *Arabidopsis* seedlings with oryzalin shows little change in the position of the nucleus. Presumably, this is due to the function of XI-I keeping the nucleus anchored to the cytoskeleton. Disrupting actin polymerization via latrunculin B treatment would also cease cytoplasmic streaming and block growth, and any related nuclear phenotype could potentially be attributed as a side effect of growth arrest (Tominaga & Kohji, 2015; Ketelaar et al., 2002). Only upon XI-I loss of function can the role of microtubules in nuclear positioning be observed. However, it is still unclear why these seemingly sophisticated nuclear positioning systems are needed in the first place, and the significance of the position of the nucleus during root hair development has yet to be elucidated.

Future Directions

Although the results presented above indicate that the disruption of microtubules results in defective nuclear positioning, there is a possibility that this is due to secondary effects. The diminished root hair growth rates observed after oryzalin treatment contradict previously published data regarding the effects of oryzalin on root hair growth, indicating secondary effects might indeed be affecting the root hairs after treatment. A simple way of determining this would be to perform a series of mock treatments, in which the initial control solution is exchanged with the same control solution instead of an oryzalin solution. It would also prove fruitful to observe the effects of varying concentrations of oryzalin on nuclear positioning and root hair growth. Further investigations into a possible linker between the nucleus and the microtubule cytoskeleton could shed more light on the complex mechanisms underlying plant nuclear movement.

References

Alonso, J.M. et al., (2003). Genome-wide insertional mutagenesis of Arabidopsis thaliana. Science 301(5633):653-657.

Bibikova T.N., Blancaflor E.B., Gilroy S. (1999). Microtubules regulate tip growth and orientation in root hairs of Arabidopsis thaliana. Plant J 17(6):657-665.

Clough S.J., Bent A.F. (1998). Floral dip: a simplified method for Agrobacterium-mediated transformation of Arabidopsis thaliana. Plant J 16(6):735-43.

Cole R.A., Fowler J.E. (2006). Polarized growth: maintaining focus on the tip. Current Opinion in Plant Biology 9, 579-588.

Haraguchi, T., Tominaga, M., Nakano, A., Yamamoto, K., Ito, K. (2016). Myosin XI-I is Mechanically and Enzymatically Unique Among Class-XI Myosins in Arabidopsis. Plant Cell Physiol, 57(8), 1732-43.

Jones, M., Smirnoff N. (2006). Nuclear dynamics during the simultaneous and sustained tip growth of multiple root hairs arising from a single root epidermal cell. J Exp Bot, 57 (15), 4269-4275.

Ketelaar, T., Faivre-Moskalenko, C., Esseling, J. J., de Ruijter, N. C. A., Grierson, C. S., Dogterom, M., & Emons, A. M. C. (2002). Positioning of Nuclei in Arabidopsis Root Hairs: An Actin-Regulated Process of Tip Growth. The Plant Cell, 14(11), 2941–2955.

Li, J., Nebenführ, A. (2007) Organelle targeting of myosin XI is mediated by two globular tail subdomains with separate cargo binding sites. Journal of Biological Chemistry 282:20593-20602.

Li, J., & Nebenführ, A. (2008). The Tail that Wags the Dog: The Globular Tail Domain Defines the Function of Myosin V/XI. Traffic, 9(3), 290-298.

Li, J., Park, E., Von Arnim, A.G., Nebenführ, A. (2009) The FAST technique: a simplified *Agrobacterium*-based transformation method for transient gene expression analysis in seedlings of Arabidopsis and other plant species. Plant Methods 5(6).

Madison, S.L., Nebenführ, A. (2013). Understanding myosin functions in plants: are we there yet? Curr Opin Plant Biol 16: 710–717

RStudio Team (2015). RStudio: Integrated Development for R. RStudio, Inc., Boston, MA URL http://www.rstudio.com/.

Schneider, C. A.; Rasband, W. S. & Eliceiri, K. W. (2012). NIH Image to ImageJ: 25 years of image analysis. Nature Methods 9(7):671-675

Starr, D.A. and Fridolfsson, H.N. (2010). Interactions between nuclei and the cytoskeleton are mediated by SUN-KASH nuclear-envelope bridges. Annu. Rev. Cell Dev. Biol. 26: 421–444.

Tamura, K., Iwabuchi, K., Fukao, Y., Kondo, M., Okamoto, K., Ueda, H., Nishimura, M., Hara-Nishimura, I. (2013). Myosin XI-i Links the Nuclear Membrane to the Cytoskeleton to Control Nuclear Movement and Shape in Arabidopsis. Current Biology, 23(18), 1776-1781.

Tominaga, M., Kojima, H., Yokota, E., Orii, H., Nakamori, R., Katayama,E., Nason, M., Shimmen, T., and Oiwa, K. (2003). Higher plant myosin XI moves processively on actin with 35 nm steps at high velocity. EMBO J. 22,1263-1272.

Tominaga, M. & Nakano A. (2012) Plant-Specific Myosin XI, a Molecular Perspective. Front Plant Sci 3, 211.

Tominaga, M. Ito, K. (2015). The molecular mechanism and physiological role of cytoplasmic streaming. Curr Opin Plant Biol 26:104-110.

Wickham, H. ggplot2: Elegant Graphics for Data Analysis. Springer-Verlag New York, 2009.

Wickham, H. (2017). tidyverse: Easily Install and Load 'Tidyverse' Packages. R package version 1.1.1. https://CRAN.R-project.org/package=tidyverse